Arch Bridges
ARCH´04
P. Roca and E. Oñate (Eds)

UPPER BOUND LIMIT ANALYSIS OF MULTISPAN MASONRY BRIDGES INCLUDING ARCH-FILL INTERACTION

A. Cavicchi[*] and L. Gambarotta[*]

[*] Department of Structural and Geotechnical Engineering
University of Genova
Via Montallegro, 1 - 16145 Genova, Italy
e-mail: gambarotta@diseg.unige.it; web page: http://prinpontimuratura.diseg.unige.it/

Key words: *Load carrying capacity, arch-fill interaction, limit analysis*

Abstract. *A numerical procedure for the limit analysis of multispan masonry bridges including the arch-fill interaction is developed based on the upper bound theorem. A two-dimensional model is defined in which arches and piers are described as beams made up of no tensile resistant (NTR), ductile in compression material, and the fill as a Coulomb material modified by a tension cut off under plane strain conditions. The model is discretized by finite elements: triangular constant strain rate elements and interface elements discretize the fill domain; the interface elements, connecting adjacent triangular elements, allow velocity discontinuities to develop; straight two-noded beam elements discretize arch and pier domains. Once the limit domains in the generalised stress space have been approximated by linear externally tangent domains, a linear programming problem is formulated and upper bounds of the collapse loads are obtained. Two examples are discussed, concerning a real single span bridge, that was subjected to a collapse test, and a three-span bridge. The effects of the fill resistance on the collapse load and the corresponding mechanism and the dependence of the load carrying capacity on the mechanical properties of fill and masonry are shown.*

1. INTRODUCTION

Collapse tests on full scale[1] and model scale[2,3,4] bridges have highlighted the strong influence of the fill and the spandrels on the collapse mechanisms and the load carrying capacity. Structural modelling of the fill-arch interaction in mechanism analysis has been considered by Crisfield[5] and Hughes *et al.* [6], in which the soil pressure is taken into account by applying additional horizontal forces to the arch; in non linear incremental FE models by Crisfield[7] and Choo *et al.* [8] the lateral resistance of the fill is modelled by a one-dimensional element, characterized by a bilinear stress strain relationship.

In this paper a numerical procedure for the limit analysis of multispan masonry bridges including the arch-fill interaction is developed based on the kinematical theorem[9]. The procedure is based on a two-dimensional finite element discretization of the masonry bridge. Arches and piers are modelled as plane beams and the fill is modelled as a continuum under plane strain conditions. The fill is discretized by triangular constant strain rate elements and the arches and piers by two-noded beams characterized by two generalized hinges at the ends; four-noded interface elements connect adjacent triangular elements in order to allow localized strains along their edges[10]. The interface elements are also used to model the interaction between the fill and the arches in order to allow concentrated strains to develop at the extrados. The constitutive model assumed for the beams is no tensile resistant (NTR) and ductile in compression, while the fill is modelled as a cohesive-frictional material according to the Coulomb hypothesis with tension cut-off.

Two examples are discussed, concerning a real single span bridge, that was subjected to a collapse test, and a three-span bridge. The results obtained by assuming heavy and resistant fill are compared with the results obtained by assuming heavy but not resistant fill. This comparison points out the effect of the fill resistance on the collapse multiplier and the corresponding collapse mechanism. Moreover, the dependence of the load carrying capacity on the mechanical parameters of the fill and of the masonry is analysed.

2. FE LIMIT ANALYSIS OF THE BRIDGE

The structural model of the masonry bridge is identified by piers, vaults and fill; vaults and piers are modelled as plane beams and the fill as a two-dimensional domain under plane strain conditions (figure 1(a)); eventual haunching is considered as fill characterized by different mechanical properties. The fill domain is discretized by three-noded triangular elements; four-noded interface elements connect the edges shared by the triangular elements in order to approximate possible discontinuities of the velocity field, as shown in figure 2. The interface elements are located also at the extrados of the arches in order to allow possible concentrated slidings; the connection between the nodes of the beams and the nodes of the interface elements of the extrados is modelled by using rigid elements[9] (figure 2).

Triangular elements have six degrees of freedom and are characterized by linear interpolation of the velocity field that allows constant strain field to develop. The interface elements have four nodes, eight degrees of freedom and linear interpolation of the velocity field; their deformation is defined by the normal and tangential components of the velocity jump along the element, so the deformation field is linear.

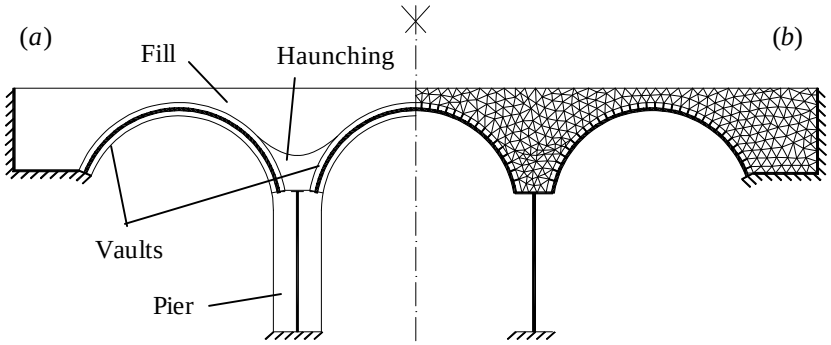

Figure 1. Finite element discretization of the bridge.

The beam element used is characterized by two generalized hinges at its ends that allow axial and rotational velocity discontinuities to develop, as shown in figure 3.

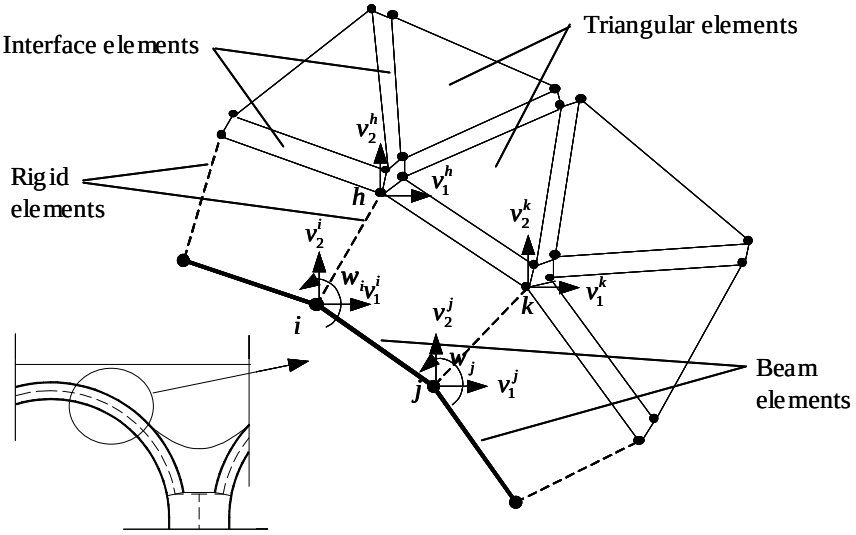

Figure 2. Particular of the discretization at the extrados.

The Coulomb admissible domain assumed for the fill is approximated by a polyhedron externally tangent in the space of stress components, defined by inequalities

$$f_k(s) = s_{11}\left(\sin j + g_1(J_k)\right) + s_{22}\left(\sin j - g_1(J_k)\right) - s_{12}\sqrt{2}g_2(J_k) - 2c\cos j \le 0, \quad k = 1...p, \quad (1)$$

being

$$g_1(J_k) = \frac{\cos J_k}{\sqrt{2\sin^2 J_k + \cos^2 J_k}}, \quad g_2(J) = \frac{2\sin J}{\sqrt{2\sin^2 J + \cos^2 J}}, \quad J_k = \frac{2p}{p}k, \qquad (2)$$

and where c is the cohesion and j the angle of internal friction. The Coulomb criterion is modified by introducing a tension cut-off condition; the corresponding domain is again linearised by a polyhedron tangent to the original domain defined by the linear inequalities

$$f_k^{lt}(s) = s_{11}\left(1+g_1(J_k)\right)+s_{22}\left(1-g_1(J_k)\right)-s_{12}\sqrt{2}g_2(J_k)-2s_t \le 0\,,\quad k=1...p\,. \qquad (3)$$

The resulting admissible domain in the stress space turns out to be the intersection of the polyhedrons defined by inequalities (1) and (3), as shown in figure 4(a).

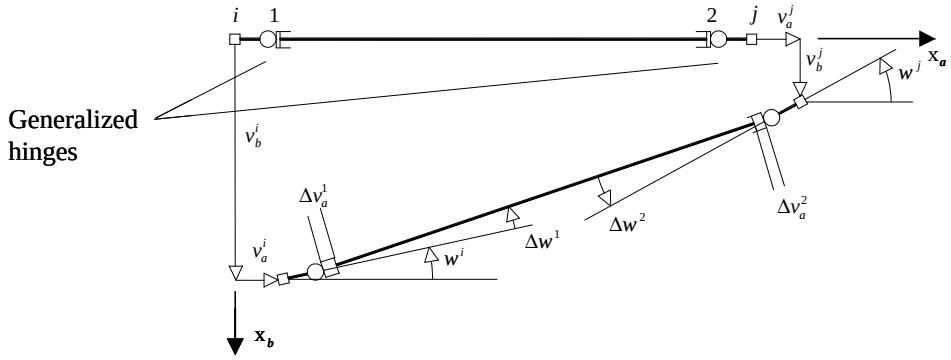

Fig. 3: Beam element.

The interface stress field is defined by the normal s_n and tangential t stress components and the admissible domain corresponds to the Coulomb criterion

$$|t_n| + s_n \tan j - c \le 0\,, \qquad (4)$$

modified by introducing the tension cut off

$$s_n - s_t \le 0\,.$$

The generalized hinges of the beam elements are characterized by the admissible domain of a rectangular section made up of a no tensile resistant and ductile in compression material. This domain, defined in the space of generalized axial and bending stress components, is linearised by a tangent polygon, as shown in figure 3(b).
All the admissible domains previously defined can be expressed by the linear inequalities

$$\mathbf{f} = \mathbf{M}^{\mathrm{T}}\mathrm{s} - \mathbf{r} \le \mathbf{0}\,, \qquad (5)$$

where the vector s collects the element generalised stress components. The associated flow rule is assumed and expressed in the matrix form

$$\dot{\mathrm{e}} = \mathbf{M}\dot{\mathrm{l}}\,,\ \dot{\mathrm{l}} \ge \mathbf{0}\,, \qquad (6)$$

where the vector $\dot{\mathrm{e}}$ collects the generalised strain rate components and vector $\dot{\mathrm{l}}$ collects the elements plastic multipliers.

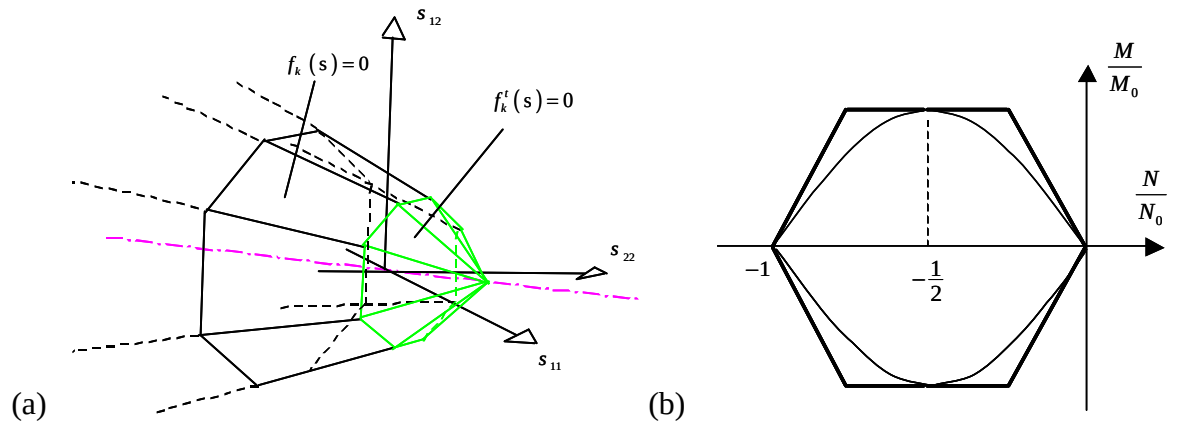

Fig. 4: Discretized admissible domains (a) of the fill and (b) of the generalized hinges.

The compatibility conditions are expressed as $\dot{\mathbf{e}} = \mathbf{B}\dot{\mathbf{a}}$, where $\mathbf{a}$ is the vector of the nodal velocities. To obtain a kinematically admissible velocity field, the compatibility conditions are imposed on the flow rule (6) thereby obtaining

$$\mathbf{B}\dot{\mathbf{a}} - \mathbf{M}\dot{\lambda} = 0, \quad \dot{\lambda} \geq \mathbf{0}. \tag{7}$$

The internal and external constraints due to the boundary conditions and the rigid links are expressed in the matrix form

$$\mathbf{A}\mathbf{a} = \mathbf{0}, \tag{8}$$

and the dissipation power P^d corresponding to the collapse mechanism takes the matrix form

$$P^d = \mathbf{r}^T \dot{\lambda}. \tag{9}$$

The applied loads are collected in the vector $\mathbf{q}$, that is decomposed as $\mathbf{q} = \mathbf{q}_0 + s\bar{\mathbf{q}}$, s being the unknown load multiplier and $\mathbf{q}_0$ and $\bar{\mathbf{q}}$ the dead and live load, respectively; the power of the external dead loads corresponding to the collapse mechanism is

$$P^e = \mathbf{q}^{0T}\dot{\mathbf{a}}. \tag{10}$$

By imposing the usual condition

$$\bar{\mathbf{q}}^T\mathbf{a} = 1, \tag{11}$$

the kinematic multiplier s_k can be expressed in the standard form as the difference between the dissipated plastic power (9) and the power of the external dead loads (10) in the form

$$s_k = P^d - P^e = \left\{ -\mathbf{q}_0^T \quad +\mathbf{r}^T \right\} \begin{Bmatrix} \dot{\mathbf{a}} \\ \dot{\lambda} \end{Bmatrix}. \tag{12}$$

The approximations introduced allow formulation of the problem of determining an upper bound for the collapse multiplier as the minimum kinematic multiplier by solving the linear programming problem

$$\begin{cases} s_k = \min\left(\mathrm{P}^d - \mathrm{P}^e\right) = \min\left\{-\mathbf{q}_0^T \quad +\bar{\mathbf{r}}^T\right\}\begin{Bmatrix}\mathbf{a}\\ \dot{\mathbf{l}}\end{Bmatrix}, \\ \begin{bmatrix}\mathbf{A} & \mathbf{0}\\ \mathbf{q}_1^T & \mathbf{0}\\ -\mathbf{B} & \mathbf{M}\end{bmatrix}\begin{Bmatrix}\mathbf{a}\\ \dot{\mathbf{l}}\end{Bmatrix} = \begin{Bmatrix}\mathbf{0}\\ 1\\ \mathbf{0}\end{Bmatrix}, \\ \dot{\mathbf{l}} \geq \mathbf{0}, \end{cases} \tag{13}$$

where the feasible domain imposes the compatibility conditions (7), (8) and condition (11).

3. EXAMPLES

3.1. Example 1: Prestwood bridge

The first example refers to Prestwood bridge[11], a single span bridge tested up to collapse within the experimental research on bridges supported by the Transport Research Laboratory (TRL) (figure 5).

Figure 5. Prestwood bridge: configuration at incipient collapse.

The geometry of the bridge is distorted. The span is 6550mm and the rise 1428mm, the vault thickness is 220mm and comprises a single ring of bricks laid as headers; the fill depth at the crown is 165mm. The load was 300mm wide and was applied across the bridge at quarter span. The configuration of the bridge just before collapse is shown in figure 5; the experimental collapse load was $\mathrm{P}_{exp} = 228\mathrm{kN}$ and the collapse mechanism exhibited four hinges. In figure 6 the collapse mechanism resulting from the numerical limit analysis is shown, obtained by assuming compressive strength $s_c = 4\mathrm{MPa}$ for the arch masonry and cohesion $c = 10\mathrm{kPa}$ and angle of internal friction $j = 37^{\circ}$ for the fill.

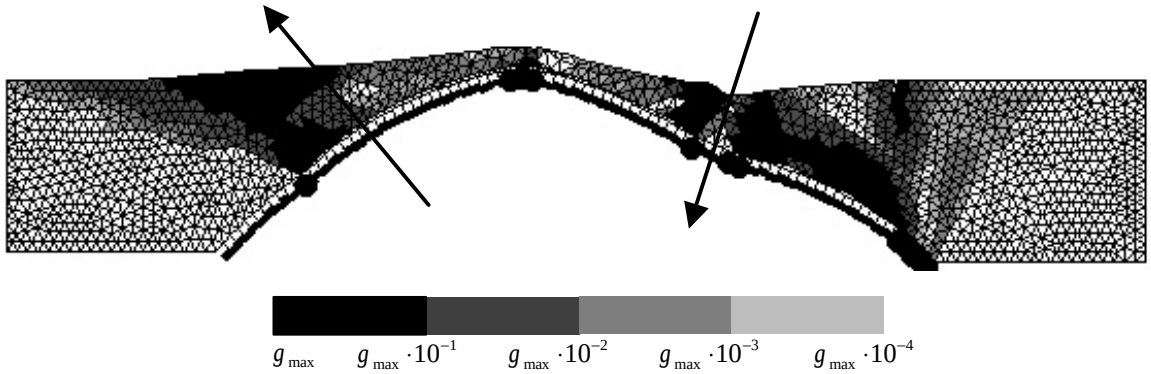

Figure 6. Collapse mechanism of the Prestwood bridge FE model.

In figure 6 the small black circles in the arch ring represent the active hinges, while the different grey areas in the fill domain correspond to different values of sliding strain rate. As in the experimental test, four groups of hinges transform the arch into a mechanism.

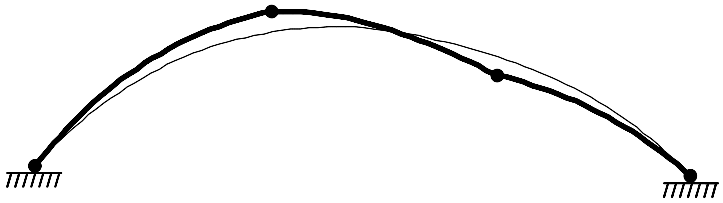

Figure 7. Collapse mechanism of the arch with no resistant fill.

This mechanism allows the loaded side of the arch to move downward, constraining the left side to widen out. As a consequence, the fill over the left side of the arch is spread over a large region up to the top surface, as shown by the left arrow in figure 6. The first hinge on the left side of the arch does not develop at the impost, as happens in a model where the fill is heavy but not resistant (figure 7); the resistance of the fill constrains the hinge to move upward.

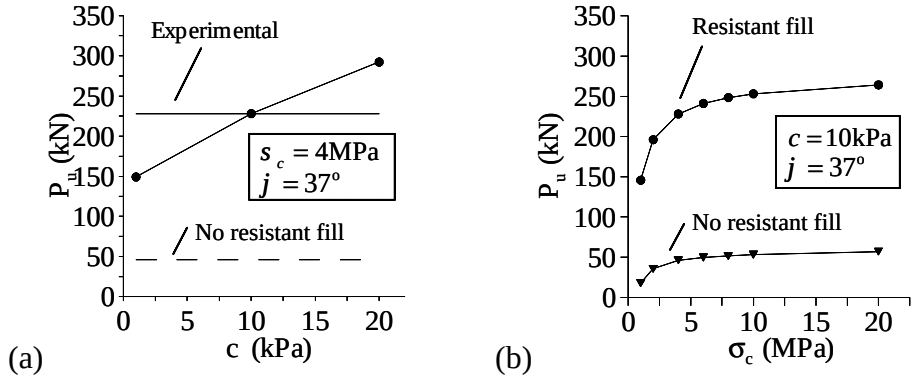

Figure 8. Influence (a) of the cohesion and (b) of the angle of internal friction on the collapse load.

The diagram in figure 8(a), obtained by assuming internal friction angle $j = 37^{o}$ and compressive strength of the arch $s_c = 4\text{MPa}$, shows the influence of the fill cohesion *c* on the collapse load; the dashed line indicates the value obtained assuming no resistant fill, $\text{P}_u = 46.2\text{kN}$. Assuming $c = 1\text{kPa}$ the collapse load is $\text{P}_u = 149.1\text{kN}$, about the 65% of the real value $\text{P}_{exp} = 228\text{kN}$ that is obtained assuming $c = 10\text{kPa}$. The diagram in figure 8(b), obtained assuming internal friction angle $j = 37^{o}$ and cohesion $c = 10\text{kPa}$, shows the influence of the compressive strength of the arch on the collapse load; the value obtained assuming unlimited compressive strength is $\text{P}_u = 267.9\text{kN}$, while the value corresponding to $s_c = 4\text{MPa}$ is $\text{P}_u = 228.0\text{kN}$; the corresponding values obtained assuming no resistant fill are $\text{P}_u = 57\text{kN}$ and $\text{P}_u = 46.2\text{kN}$ respectively.

3.2. Example 2: Three-span bridge

The three-span bridge considered has circular arches, having 1m thickness, 7m internal radius and span to rise ratio equal to 2. The height of the piers is $\text{h} = 10\text{m}$ and the thickness is $\text{h}_p = 3\text{m}$; the internal radius of the arch is R_{int}= 7m and the thickness is $\text{h}_a = 1\text{m}$; the depth of fill at crown is $\text{h}_f = 1\text{m}$. The assumed material parameters are: fill density $g = 18\ KN/m^3$, cohesion $c = 20\text{kPa}$, angle of internal friction $j = 30^{o}$. The dead loads are due to the weights of the fill and of the arch, while the live load corresponds to a triangular symmetric pressure distribution 6m wide at the midspan (figure 9).

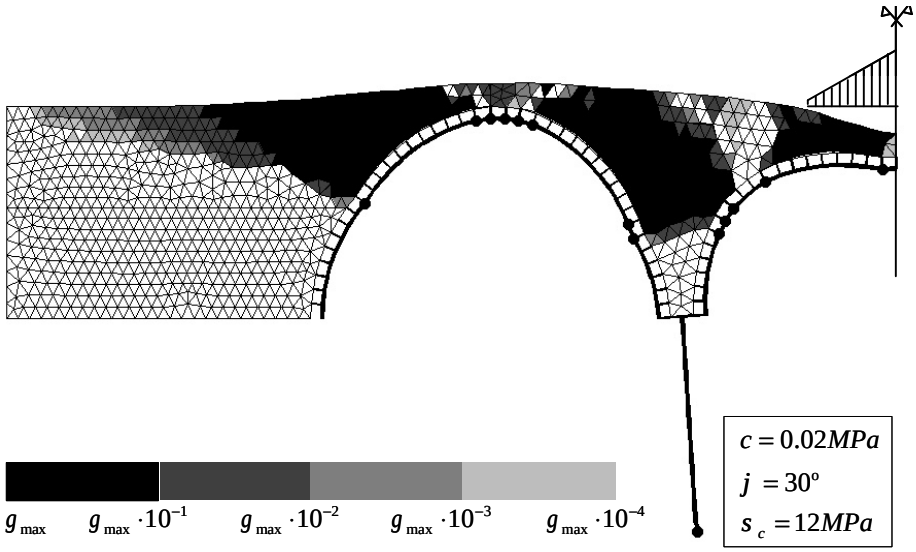

Figure 9. Collapse mechanism of the three-span bridge.

In the following, model A is referred to the model in which the fill is heavy and resistant and model B to the model where the fill is assumed heavy but not resistant; model C is defined with the same assumptions as model B, but the haunching is modelled as a rigid body. In figure 9 the collapse mechanism of model A is shown, where the arch-pier-fill interaction is clearly represented. The failure mechanism of the arch-pier system is characterised by thirteen groups of hinges attained at the crowns and at the haunches of the arches and at the bottom sections of the piers.

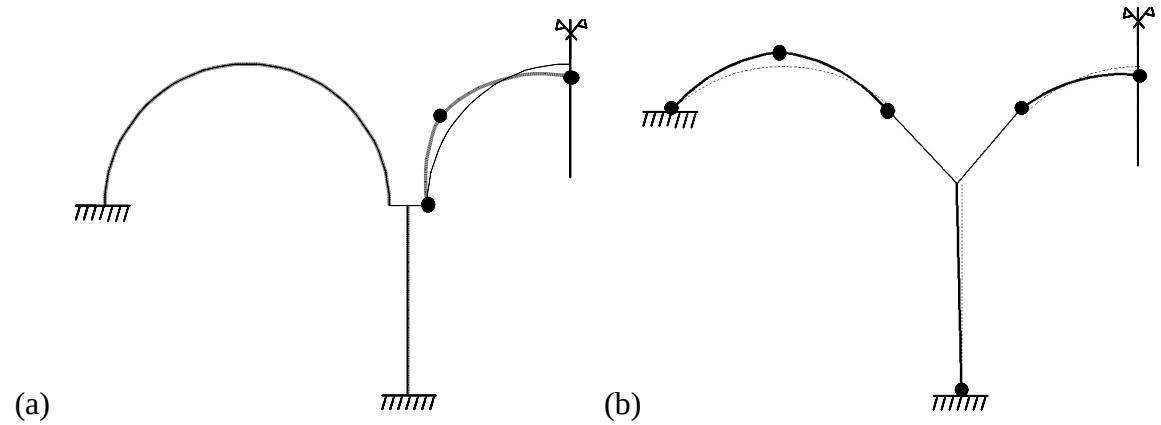

Figure 10. The collapse mechanisms of model B and model C.

This mechanism allows the crown of the central arch to move downward imposing the rotation of the piers and the contraction of the lateral arches, in which the crowns move upward; a compatible inelastic deformation field is attained in the fill, that is constrained to move upward. Inelastic sliding is spread over a large region of the fill that extends beyond the ends of the external arches. In figures 10 (a) and (b) the collapse mechanisms of model B and model C are shown, respectively; the collapse mechanism of model B is limited to the central arch, so it behaves as a single arch bridge.

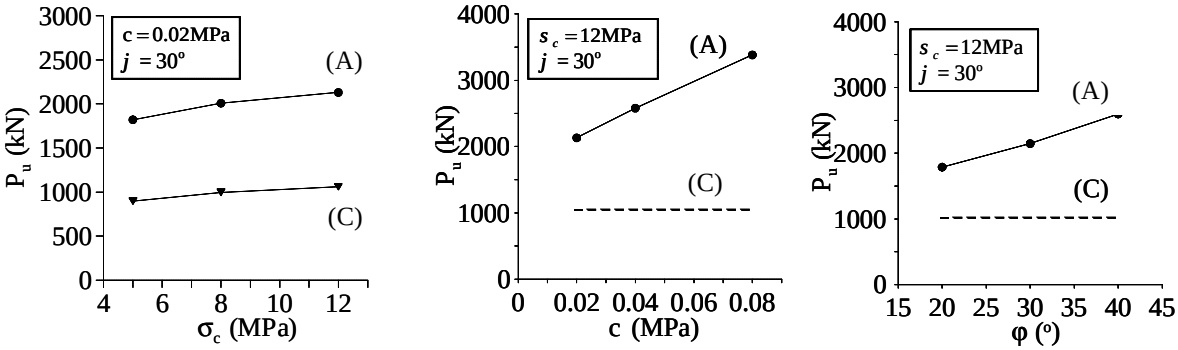

Figure 11. Influence of the mechanical parameters of the masonry and fill on the collapse load.

The diagram in figure 11a shows the dependence of the failure load carrying capacity on the compressive strength in models A and C. The values from model A turn out to be about 2

times as great as the corresponding values of model C. The diagrams in figure 11 (b) and (c) show the dependence of the load carrying capacity on the values of the cohesion and of the angle of internal friction in the models A; the dashed line corresponds to model C.
The results obtained seem to be encouraging, although the limits of the model are evident: plane strain condition is a strong approximation whose effects have to be investigated and the modelling of velocity discontinuities has to be improved by more specific interpolations.

4. CONCLUSIONS

The effect of the fill on the collapse behaviour of masonry bridges can be relevant, as experimental results show. The numerical procedure described in this paper, based on the kinematical theorem of limit analysis, allows one to obtain the collapse mechanism and the corresponding load multiplier of an FE model in which the fill is considered heavy and resistant. The two examples show the good capacity of the procedure to describe the behaviour of the bridge resulting from the arch-fill interaction. In particular the first example, concerning a real bridge tested to collapse, has shown good agreement of the numerical results with the real collapse behaviour of the bridge. The second example concerning a three-span bridge has shown the capability of the procedure to represent complex interaction between piers, arches and fill at collapse. In both examples the influence of fill and masonry parameters has been analysed; the collapse loads obtained by varying the cohesion and the angle of internal friction of the fill have shown that the fill mechanical properties can increase the load carryinig capacity of the bridge significantly.

REFERENCES

[1] Page J., Masonry Arch Bridges - TRL State of the Art Review, HMSO, 1993.
[2] Royles R. e Hendry A.W., Model tests on masonry arches, *Proc. Instn Civ. Engrs*, Part 2, 91, 299-321, 1991.
[3] Melbourne C., Walker P.J., Load Tests to collapse of model brickwork masonry arches, Proc. 8th International Brick and Block Masonry Conference, vol. 2, New York: Elsevier Applied Science, pp. 991-1002, 1988.
[4] Hughes T.G., Davies M.C.R., Taunton P.R., The influence of soil and masonry type on the strength of masonry arch bridges, *Proc. Sec. Int. Arch Bridge Conf.,* A. Sinopoli Ed., 321-330, 1998.
[5] Crisfield M.A., Packam A. J., A mechanism program for computing the strength of masonry arch bridges. Transport Research Laboratory, Crowthorne, Research Report 124, 1985.
[6] Hughes T.G., Hee S. C., Soms E., Mechanism analysis of single span masonry arch bridges using a spreadsheet, *Proc.Inst. Civ. Eng. Struct. Build.,* 152, 341-350, 2002.
[7] Crisfield M.A., Finite element and mechanism methods for the analysis of masonry and brickwork arches, Transport Research Laboratory, Crowthorne, Research Report 19, 1985.
[8] Choo B. S., Coutie M. G., Gong N. G., Finite element analysis of masonry arch bridges using tapered elements, *Proc. Instn. Civ. Engrs.*, Part 2, 91, Dec. 755-770, 1991.
[9] Cavicchi A., Gambarotta L., Limit Analysis of multispan masonry bridges including arch-fill interaction, STRUMAS VI Computer Methods in Structural Masonry, 22nd-24th September 1993.
[10] Sloan S.W., Kleeman P.W., Upper bound limit analysis using discontinuous velocity fields, *Comp. Methods Appl. Mech. Engrg*, **127**, 293-314, 1995.
[11] Page J., Load tests to collapse on two arch bridges at Preston, Shropshire and Prestwood, Staffordshire, Department of Transport, TRRL Research Report 110, TRL, Crowthorne, England, 1987.